# An approach to prediction and providing of compression ratio for DCT-based coder applied to remote sensing images

R. A. Kozhemiakin[1], A. N. Zemliachenko[1], V. V. Lukin[1*], S. K. Abramov[1], B. Vozel[2]

[1] *National Aerospace University, Kharkov, Ukraine*

[2] *University of Rennes 1, Lannion, France*

A novel compression ratio prediction and providing technique applicable to noisy and almost noise-free remote sensing images is proposed. It allows predicting and then providing a desired compression ratio for DCT-based coder in automatical manner. The proposed technique is algorithmically simple and has low computational complexity that allows using it onboard spaceborne or airborne carriers. The study is carried out for test and real-life Hyperion images. It is shown that the proposed technique has high accuracy and it is robust with respect to noise intensity and type. Relative error of prediction of providing compression ratio does not exceed 10%.

**Keywords:** remote sensing, DCT-based coders, compression ratio prediction, hyperspectral data

## Introduction

Nowadays, compression techniques become very important due to increasing amount of data acquired by new generations of remote sensing satellites, modern camcorders, cameras and other imaging processing systems [4, 7]. Wherein, acquired images typically contain spatial and spectral (for multichannel and hyperspectral images) redundancy [3, 21] and they should be transmitted via telecommunication channels and/or stored. Most lossless compression techniques cannot provide the compression ratio (CR) more than 3...5 times and even less if an image is highly textured and/or distorted by noise [19, 15].

Near-lossless or lossy compression techniques can provide a considerably higher CR (lossy techniques are able to produce CR values up to 100 or even higher) [14, 17] but the main question in compression of remote sensing data is how to provide a desired CR with acceptable image quality (according to standard criteria or visual quality metric)?

In the widespread JPEG image coder, there is a simple and not perfect option to control quality of a compressed image [16]. A low-quality image is associated with a smaller JPEG image size whilst for high-quality image a larger image size (smaller CR) is needed [11]. However, unfortunately, in the standard JPEG version, there is no possibility to provide a desired CR. A desired CR can be provided with the newer standard JPEG2000 or by the coder SPIHT [13] but the same bit rate for different images can result in different visual qualities. It is possible to use iterative procedures that presume image multiple compression/decompression with control of CR or other metric at each step [10]. An obvious disadvantage of such procedures is that they might require extensive computations.

Another way is to control CR or bit rate by some model parameter dependence of CR on quantization step or other model parameter [6, 5]. In this article, we focus on predicting CR and providing a desired CR for compressing noisy optical remote sensing images under assumption that lossy DCT-based coder AGU [12] is used.

## General CR prediction technique

It is well known that a larger number of zeros in an image after applied orthogonal transform and coefficient quantization leads to a higher CR-this fact is met and used in many already designed lossy compression techniques [1].

The CR prediction technique proposed by us in [20] and modified below is based on this fact, too. We show that CR can be predicted based on input statistical parameter $P_0$ (percentage of zeros after DCT and quantization) computed in a set of $8 \times 8$ pixel blocks. In this way, it is possible to approximately estimate percentage of zeros in a transformed image that can be used as an input parameter of an analytical prediction curve. In other words, prediction implies that one estimates $P_0$ for a given image and then substitutes this parameter into already known dependence as argument. The output value is an estimate (prediction) of CR or bpp [20, 18].

Analytical prediction dependence can be obtained by curve fitting into a scatter-plot of pairs CR or bpp on $P_0$ computed for a large set of test images corrupted by noise for a used coder [18]. Examples of such scatter-plots and fitted curves for CR and bpp are given in Fig. 1 and 2.

A good prediction is possible if a scatter-plot is "compact" (its points are placed close to a fitting curve) and this curve is fitted properly. Then, fitting and prediction can be characterized by certain quantitative criteria (parameters) where goodness of fits $R^2$ [2] is, probably, one of the most often used ones. In the case
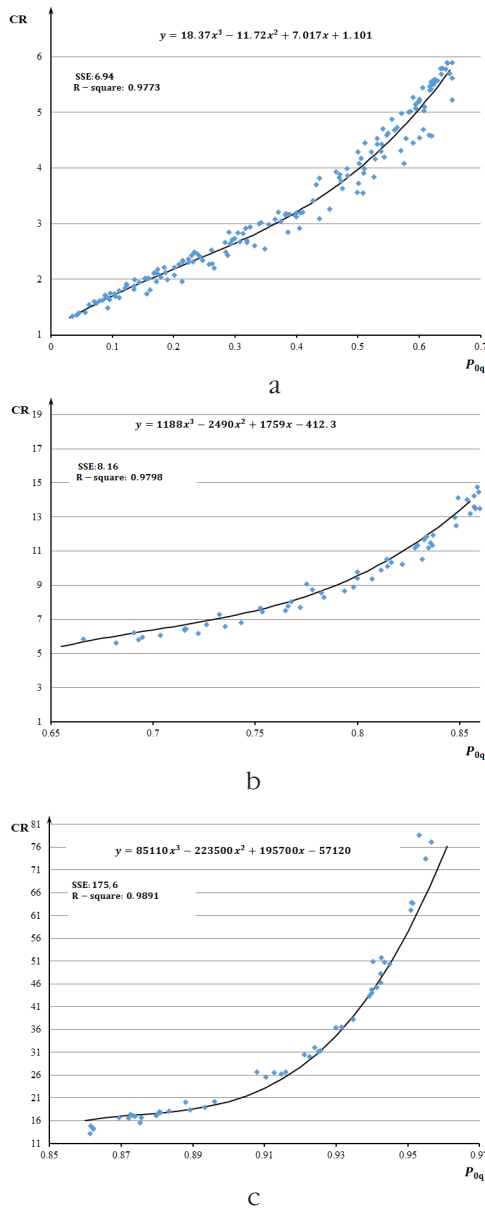
a



b



c

**Fig. 1.** Scatter-plot of CR vs. $P_0$ for test images corrupted by AWGN with different values of noise variance with three variants of curve fitting for the coder AGU for the interval [0; 0.65] (a), for the interval (0.65; 0.85] (b), for the interval (0.85; 1] (c)

of compact scatter-plot and proper fitting $R^2$ tends to unity. In all the cases in Figures 1 and 2, $R^2$ exceeds 0.97. This means that fitting is good enough [2].

Note that prediction procedure should be accurate and fast enough. Accuracy is partly characterized by the aforementioned parameter $R^2$ and will be discussed below. In turn, computational load of prediction is low. One needs to have non-overlapping $8 \times 8$ pixel blocks with their total number about 500. If a given image size allows obtaining more non-overlapping blocks, 500 blocks can be chosen randomly. Then, availability of fast 2D DCT algorithms (implemented in software or hardware) allows prediction to be done considerably faster than compression (see additional details below).

There are certain assumptions and requirements

concerning formed scatter-plots and fitted curves. First of all, the arguments of a scatter-plot should cover entire range of possible variation of a considered input parameter. For the studied probability $P_0$, this range is theoretically from 0 to 1. Second, this range should be covered quite densely and with approximately equal density in its subintervals to provide quite accurate fitting. These two requirements (recommendations) have been fulfilled by using a great number of test images of different complexity corrupted by additive white Gaussian noise (AWGN) of different intensity and compressed using a wide set of QS values.

Third, the fitted curve has to have reasonable (expected) behavior. In particular, from experience in [5, 20, 18, 9] one can expect that CR monotonically increases if $P_0$ becomes larger. Besides, CR should not be smaller than 1 for a prediction curve for $P_0$ approaching to 0.

These requirements have been taken into account in curve fitting into the scatter-plot CR vs $P_0$. It occurred that fitting the only one (common) function for entire range of $P_0$ variation does not allow satisfying these requirements easily (exponential and polynomial functions have been tried). Therefore, we have divided the full range of $P_0$ variation into three intervals as shown in Fig. 1. This has allowed providing good fitting by quite simple third order polynomials with high values of $R^2$ for each interval.

Similar approach has been used for approximating the dependence of bpp on $P_0$ (Fig. 2). Clearly, bpp monotonically reduces if $P_0$ increases. Whilst the dependence for rather large $P_0$ is almost linear as in [5] for different orthogonal transform based compression techniques, the dependence is obviously nonlinear for $P_0$ smaller than 0.65. This has motivated us to use two intervals (see Fig. 2).

Consider now the parameter $P_0$. Having $Q$ analyzed $8 \times 8$ pixel blocks, the probability $P_0$ is determined as

$$P_0 = \frac{1}{63} \sum_{q=1}^{Q} \sum_{r=0}^{7} \sum_{s=0}^{7} \delta(q,r,s) \qquad (1)$$

$$\delta(q,r,s) = \begin{cases} 1, if \left| D(q,r,s) \right| < 2QS \\ 0, otherwise \end{cases} \qquad (2)$$

where $D(q, r, s)$, $r = 0,...,7$; $s = 0,...,7$; $q = 1,...,Q$; is rs-th DCT coefficient determined in $q$-th analyzed block of size $8 \times 8$ pixels.

Knowing $P_0$ for a given QS and an image to be compressed, one can predict CR or bpp quite accurately. However, often the task is not to predict CR or bpp but to solve slightly inverse task – to determine what QS to use in order to provide a desired CR or bpp.

## Proposed methodology of providing a desired CR

In this research, we obtain and analyze data for the DCT-based coder AGU [12] that carries out image compression in non-overlapping $32 \times 32$ pixel blocks and
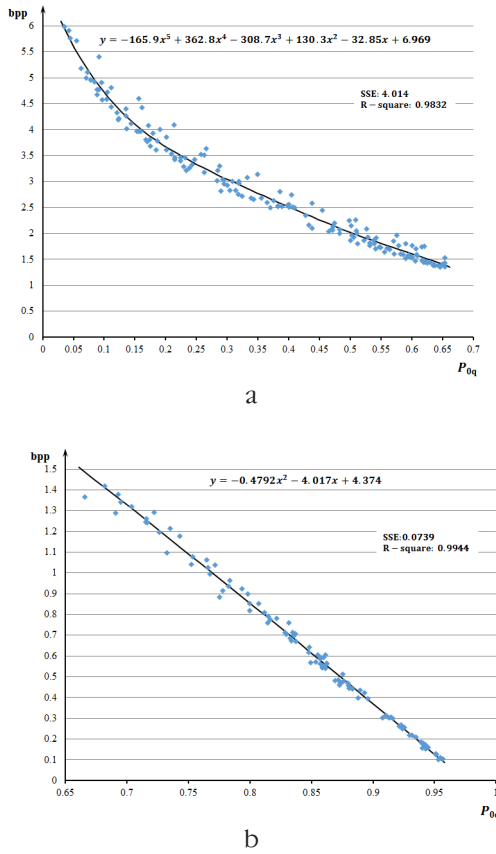
a



b

**Fig. 2.** Scatter-plot of bpp vs. $P_0$ for test images corrupted by AWGN with different values of noise variance with three variants of curve fitting for the coder AGU for the interval [0; 0.65] (a), for the interval (0.65; 1.0) (b)

deblocking after decompression. It performs better than JPEG and slightly better than JPEG2000 [12]. CR for AGU is controlled by QS – a larger $QS$ results in a larger CR.

Below we describe the proposed methodology of providing a desired CR $CR_{des}$. It is the following (see the algorithm structure in Fig. 3 for the CR case). At the first step, DCT-coefficients are calculated for a chosen set of $8 \times 8$ pixel non-overlapping blocks (at least, 500).

At the second step, only the obtained positive DCT-coefficients are considered where block mean (DC) DCT coefficients (where $D(q, r, s)$, $q = 1,...,Q$) are excluded from analysis. Consideration of only positive DCT-coefficients takes into account the fact that AC DCT-spectrum is symmetrical (see examples of the histograms in Fig. 4) and then it becomes possible to work with its positive half for processing boosting. Thus, one constructs the positive AC DCT coefficient histogram and gets pairs $V$-$F$ of DCT-coefficient values $V$ ($V = 0,...,\max(V)$) and their frequencies $F$.

We have analyzed quite many test images, noise intensities, values of initial quantization step $QS_0$ and ways to present histograms. Based on the obtained experience, we propose using histograms with integer values

for favoring the algorithm simplicity. For this purpose, the DCT-coefficients originally presented as floating point values are rounded to integers.

It should be noted that for providing the highest accuracy the rounding must be carried out to the nearest integer towards zero. After quantization, usual rounding to the nearest integer is performed. Next, quantize $V$ with some $QS_0$ and compute $P_0$ (percentage of zeros) as

$$P_0 = F(0) + 2 \sum_{V=1}^{V_{max}} \frac{if\ round(F(V)/QS_0) = 0}{63Q}, \quad (3)$$

where $F(0)$ denotes the first histogram row and contains number of zeros in all processing blocks; $F(V)$ denotes the number of other DCT-coefficients.

Then, compute (with a priori obtained prediction curve) a predicted CR using expressions (4), (5) and (6) (or bpp using expressions (7) and (8)) given below. For CR prediction, the dependence (for $P_0$ range [0; 0.65]) is the following

$$CR_p(P_0) = 18.37 \cdot (P_0)^3 - 11.72 \cdot (P_0)^2 + 7.017 \cdot (P_0) + 1.1. \quad (4)$$

If $P_0 \in (0.65; 0.85]$, then

$$CR_p(P_0) = 1188 \cdot (P_0)^3 - 2490 \cdot (P_0)^2 + 1759 \cdot (P_0) - 412.3. \quad (5)$$

And for $P_0 \in (0.85; 1]$, the prediction curve is

$$CR_p(P_0) = 85110 \cdot (P_0)^3 - 223500 \cdot (P_0)^2 + 195700 \cdot (P_0) - 57120. \quad (6)$$

For the bpp case: if $P_0 \in [0; 0.65]$, then

$$bpp_p = -165.9 \cdot (P_0)^5 + 362.8 \cdot (P_0)^4 - 308.7 \cdot (P_0)^3 + 130.3 \cdot (P_0)^2 - 32.85 \cdot (P_0) + 6.969, \quad (7)$$

and if $P_0 \in (0.65; 1]$, then the approximation is

$$bpp = -0.4792 \cdot (P_0)^2 - 4.017 \cdot (P_0) + 4.374. \quad (8)$$

If the computed $CR_p$ value is less than $CR_{des}$, then increase QS (decrease it vice versa) and compute $P_0$ again. Operations are repeated until a desired value of $CR$ is reached (see block-diagram in Fig. 3).

Accuracy of the described method and algorithm as well as its computational complexity depend upon several factors as how a histogram has been constructed, what is $QS_0$ used, how QS is changed (what is its increment), what is a desired CR, what is complexity of an image to be compressed and noise intensity in it? Comparison of the DCT-coefficient histograms in Fig. 4 for two values of additive noise variance show that even for the same image (but different noise intensity) the distributions are quite different. Then, the
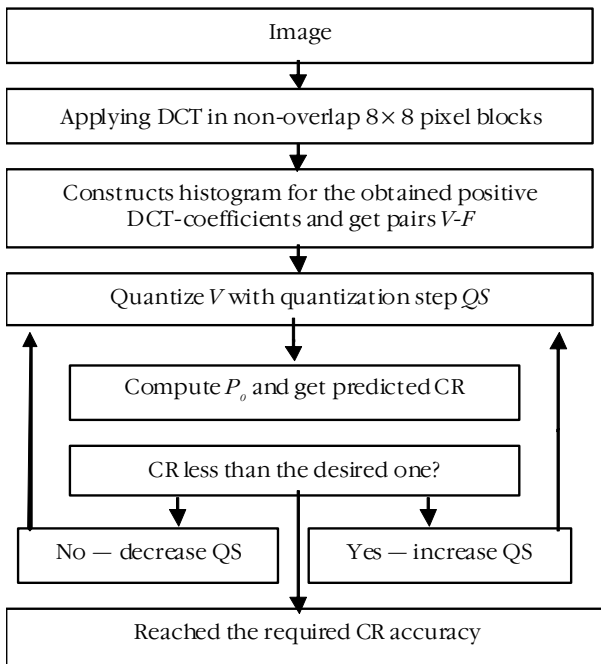
**Fig.3.** The proposed algorithm of desired CR providing

use of the same QS results in different $P_0$ and, respectively, CR.

The peculiarity of the proposed methodology is that the described iterative procedure for CR providing does not require any compression/decompression of images and operates only with the histogram values V that have many times less size than the image size. In addition, the proposed methodology is very simple and has low computational complexity. Only arithmetic and logical operations are employed. The recommended start $QS_0$ is equal to 20 for compressing images represented as 8-bit 2D data array.

### Analysis of prediction accuracy for test images

Consider the situation for three standard test gray images typical for remote sensing (Fig. 5) distorted by AWGN with different noise variance values (they were in wide limits but below we study the results for variance values equal to 25 and 65). The obtained results for different QS are presented in Table 1.

Let us start from the simplest case of the simple structure test image Frisco (Fig. 5, c) corrupted by AWGN with variance 25. As it seen from analysis of the presented data, for all studied QS values the predicted value of CR is slightly less (by about 1.02 times or by 2%) than the practically attained CR. The situation is similar for bpp, predicted values are slightly larger than the corresponding actual ones. For the case variance = 65, the technique has provided accurate outputs for both CR and bpp and the largest relative estimation error is 13%.
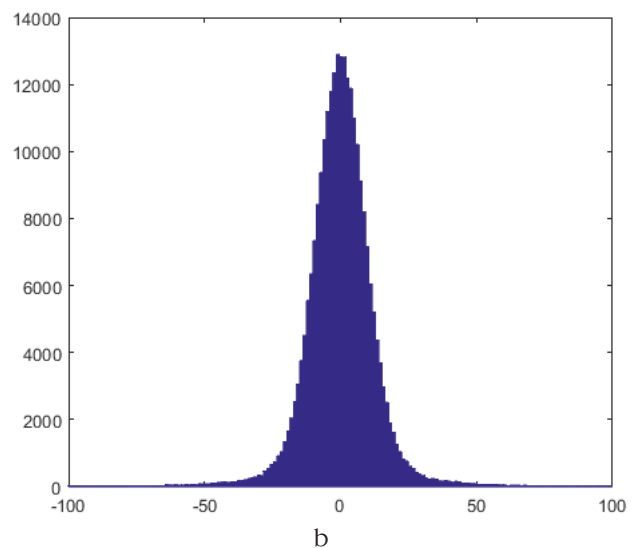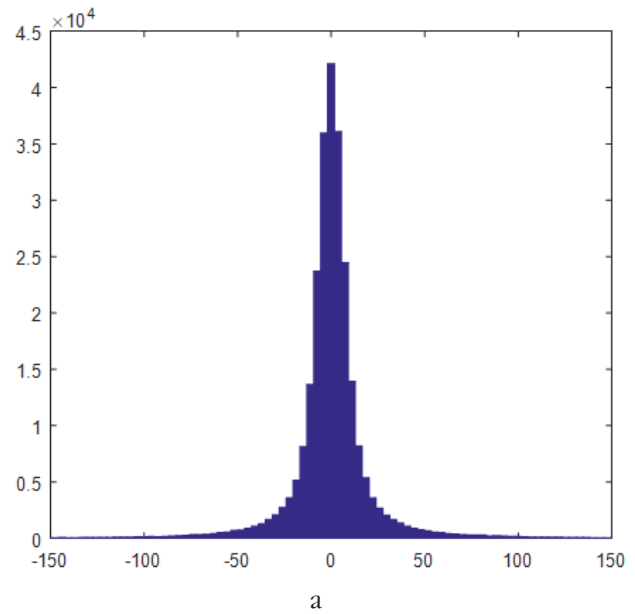


**Fig. 4.** Histogram of DCT-coefficients for image Aerial corrupted by AWGN with variance = 25 (a) and variance = 65 (b)

Consider now the case of more complex structure (textural) test images Aerial and Airfield (Fig. 5, a, b). For the test image Aerial (variance = 25), the predicted bpp value practically coincides with the values attained in practice. For the test image Airfield the largest difference is 6%. For CR case, the maximal relative error does not exceed 7%. For variance = 65 the obtained results are similar. It should be noted that the noise level does not affect the accuracy of predictions. It is confirmed by comparing the obtained results for two values of AWGN variance (Table 1). Meanwhile, the proposed approach is able to perform for other noise types as well (this has been checked by us). The reason is that the parameter $P_0$ in no way takes noise type and variance into account and deals only with DCT coefficient statistics.

**Fig. 5.** Test images (from left to right) Aerial (a), Airfield (b), Frisco (c)

**Table 1**
Obtained CR and predicted CR values for the considered test images

| Image | QS | $P_0$ | $CR_{predicted}$ | $CR_{real}$ | $bpp_{predicted}$ | $bpp_{real}$ |
|---|---|---|---|---|---|---|
| | | | Variance = 25 | | | |
| Aerial | 10 | 0.40 | 3.21 | 3.18 | 2.50 | 2.52 |
| | 20 | 0.65 | 5.27 | 5.10 | 1.56 | 1.57 |
| | 30 | 0.76 | 7.95 | 7.81 | 1.04 | 1.02 |
| Airfield | 10 | 0.34 | 2.85 | 3.01 | 2.82 | 2.66 |
| | 20 | 0.59 | 4.93 | 4.61 | 1.65 | 1.74 |
| | 30 | 0.74 | 7.24 | 6.97 | 1.13 | 1.15 |
| Frisco | 10 | 0.52 | 4.16 | 4.29 | 1.93 | 1.86 |
| | 20 | 0.80 | 9.56 | 9.59 | 0.85 | 0.83 |
| | 30 | 0.89 | 18.56 | 19.04 | 0.42 | 0.42 |
| | | | Variance = 65 | | | |
| Aerial | 10 | 0.32 | 2.75 | 2.90 | 2.93 | 2.76 |
| | 20 | 0.55 | 4.47 | 4.36 | 1.81 | 1.83 |
| | 30 | 0.71 | 6.58 | 6.35 | 1.28 | 1.26 |
| Airfield | 10 | 0.29 | 2.60 | 2.82 | 3.10 | 2.84 |
| | 20 | 0.52 | 4.16 | 4.19 | 1.93 | 1.91 |
| | 30 | 0.69 | 6.19 | 5.83 | 1.37 | 1.37 |
| Frisco | 10 | 0.39 | 3.14 | 3.55 | 2.56 | 2.25 |
| | 20 | 0.67 | 5.80 | 5.90 | 1.47 | 1.36 |
| | 30 | 0.83 | 11.59 | 12.02 | 0.71 | 0.67 |

**Analysis of prediction accuracy for real-life images**

For verification of the considered approach, real-life Hyperion images have been used (Fig. 6). It should be noted that Hyperion images are corrupted by a more complex noise than AWGN [19]. In fact, the observed noise is the sum of signal-dependent and AWGN components. Besides, the original images are 16-bit data. Therefore, we have applied variance-stabilizing transform (VST) [8] with parameters based on pre-estimated noise parameters (signal-dependent (SD) and signal-independent (*SI*) parameters) that converts noise into additive and makes data dynamic range narrower (8-bit). For analysis, we have taken three images from two sets (image 1 and image 2 were cut from EO1H1800252002116110KZ set, the image 3 was cut from EO1H2010262004157110KP set) from the 221-th channel of these datasets.

The analysis of data presented in Table 2 shows the following:
1) for all images the predicted bpp values for QS = 5 are practically the same as the corresponding values obtained in practice;
2) for QS = 5 and QS = 10, relative errors of prediction do not exceed 8%;
3) for the CR values predicted for QS = 15, the prediction accuracy is also high and relative error does not exceed 2–3%;
4) for the QS = 5 and QS = 10 cases, the situation with predicting bpp is very similar.

**Analysis of accuracy for desired CR providing**

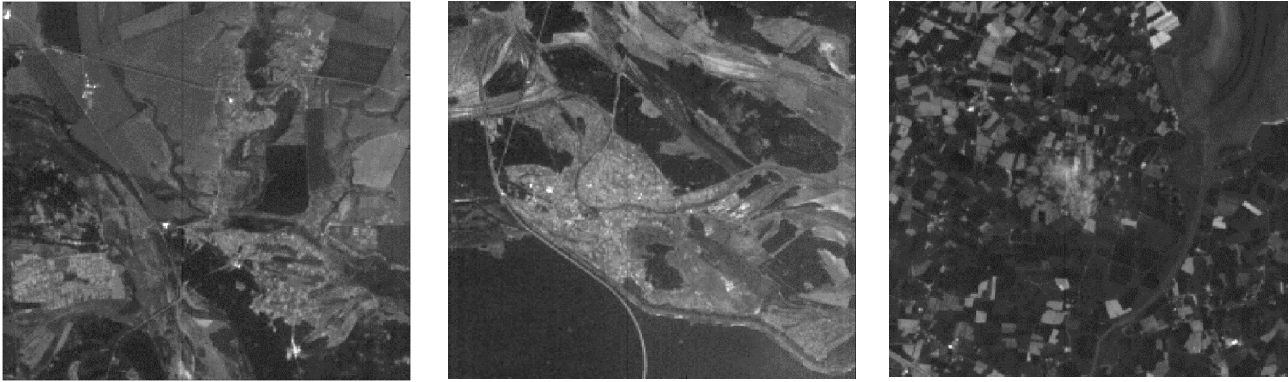The goal of the iterative procedure described earlier is to find QS that satisfies specified accuracy

**Fig.6.** Real-life Hyperion images (Im1, Im2, and Im3 from left to right)

**Table 2**
Obtained CR and predicted CR values for Hyperion images

| Image | QS | $P_0$ | $CR_{predicted}$ | $CR_{real}$ | $bpp_{predicted}$ | $bpp_{real}$ |
|---|---|---|---|---|---|---|
| | | Channel (sub-band) № 221 (wavelength = 2365 nm), $SI_{variance} = 16$ $SD_{parameter} = 0.03$ | | | | |
| Im1 | 5 | 0.44 | 3.48 | 3.61 | 2.30 | 2.21 |
| | 10 | 0.68 | 6.40 | 6.25 | 1.42 | 1.28 |
| | 15 | 0.82 | 10.83 | 10.51 | 0.76 | 0.76 |
| Im2 | 5 | 0.43 | 3.44 | 3.71 | 2.34 | 2.15 |
| | 10 | 0.69 | 6.24 | 6.53 | 1.37 | 1.22 |
| | 15 | 0.82 | 10.83 | 10.96 | 0.75 | 0.72 |
| Im3 | 5 | 0.44 | 3.49 | 3.74 | 2.30 | 2.13 |
| | 10 | 0.70 | 6.57 | 6.63 | 1.33 | 1.20 |
| | 15 | 0.83 | 11.59 | 11.04 | 0.71 | 0.72 |

between desired and provided. There are several sources of errors. The first is in prediction using the fitted curves. As it follows from data in Fig. 1 and 2, CR for each image can slightly differ from a value predicted via approximation. Second, $P_0$ can be estimated with some error due to limited number of analyzed blocks. Third, QS can be determined with some error. Errors due to the first source are predominant. To decrease the third source error, it is possible to determine QS better using two QS values that provide CR closest to its desired value (from both sides of final QS). To do this, we propose employing simple linear interpolation

$$QS_{ip} = QS_{ls} + \frac{QS_{dr} - QS_{pls}}{QS_{phs} - QS_{ipls}}(QS_{hs} - QS_{ls}) , \qquad (9)$$

where $QS_{ip}$ is the final (interpolated) QS, $CR_{dr}$ denotes the desired CR, $CR_{pls}$ is the predicted CR computed form lower side of the desired CR for $QS_{ls}$, $CR_{phs}$ is the predicted CR value computed from the higher side of the desired CR for $QS_{hs}$.

Consider now the results obtained in this way. Let us start from the test image Aerial (corrupted by AWGN with noise variance 25) for which it is supposed necessary to provide, for example, $CR_{des} = 5$ (see data in Table 3). From the lower side of the desired value, we have obtained the predicted $CR_{pls} = 4.68$ for $QS_{ls} = 16$ whilst from higher side the predicted $CR_{phs} = 5.19$ for $QS_{hs} = 17$. As a result, the use of the obtained interpo-

lated value $QS_{ip} = 16.63$ has provided $CR_{real} = 4.46$ (with relative error 12%). For the case of variance = 65, the relative error of the provided CR is less or equal to 8%. Parameters of the algorithm for other test images and the obtained data are given in Table 3. As it can be seen, the difference between the desired and provided CR values does not exceed 10%. For less complex image Frisco, the desired CR is provided with smaller value of QS. We have also obtained and considered the results for real-life Hyperion images. As it is seen from the analysis of data in Table 4, the proposed technique provides accurate CR values, too. For the chosen desired $CR_{des} = 7$, the designed method produce CR values with relative error less than 10%.

**Conclusions**

The automatic method of CR/bpp prediction for DCT-based coder AGU is described and verified for test and real-life Hyperion images corrupted by additive noise. It is shown that CR/bpp value can be predicted with high accuracy where relative error usually does not exceed 13%. Moreover, the algorithm for providing a desired CR is designed. It is also tested and shown to be accurate as well.

The proposed method is algorithmically simple and has low computation complexity. In future, we plan to consider more complex models of noise and multichannel images.

**Table 3**
Provided CR values with proposed technique for the considered test images

| Image | Variance | $QS_{ls}$ | $QS_{hs}$ | $CR_{pls}$ | $CR_{phs}$ | $QS_{interpolated}$ | $CR_{des}$ | $CR_{real}$ |
|-------|----------|-----------|-----------|------------|------------|---------------------|------------|-------------|
| Aerial | 25 | 16 | 17 | 4.68 | 5.19 | 16.63 | 5 | 4.46 |
|        | 65 | 30 | 31 | 6.78 | 7.19 | 30.54 | 7 | 6.47 |
| Airfield | 25 | 20 | 21 | 4.93 | 5.49 | 20.13 | 5 | 4.78 |
|          | 65 | 32 | 33 | 6.63 | 7.14 | 32.73 | 7 | 7.67 |
| Frisco | 25 | 10 | 11 | 4.16 | 5.05 | 10.94 | 5 | 4.57 |
|        | 65 | 22 | 23 | 6.80 | 7.51 | 22.28 | 7 | 6.65 |

**Table 4**
Provided CR values with proposed technique for Hyperion images

| Image | $QS_{ls}$ | $QS_{hs}$ | $CR_{pls}$ | $CR_{phs}$ | $QS_{interpolated}$ | $CR_{desired}$ | $CR_{real}$ |
|-------|-----------|-----------|------------|------------|---------------------|----------------|-------------|
| Im1 | 10 | 11 | 6.40 | 7.46 | 10.57 | 7 | 6.63 |
| Im2 | 10 | 11 | 6.24 | 7.79 | 10.49 | 7 | 6.79 |
| Im3 | 10 | 11 | 6.57 | 7.95 | 10.31 | 7 | 6.78 |

# References

1. Al-Chaykh O. K. Lossy compression of noisy images / O. K. Al-Chaykh, R. M. Mersereau // IEEE Transactions on Image Processing. — 1998. — Vol. 7 (12). — P. 1641–1652.

2. Cameron C. An R-squared measure of goodness of fit for some common nonlinear regression models / C. Cameron, A. Windmeijer, A. G. Frank, H. Gramajo, D. E. Cane, C. Khosla // Journal of Econometrics. — 1997. — Vol. 77. — № 2. — P. 329–342.

3. Chang C-I. Hyperspectral Data Processing: Algorithm Design and Analysis. First Editions / C-I. Chang // John Wiley and Sons, Inc. — 2013. — 1164 p.

4. Christophe E. Hyperspectral Data Compression Tradeoff / E. Christophe // Optical Remote Sensing. Advances in Signal Processing and Exploitation Techniques, Springer. — 2011. — Vol. 8. — P. 9–29.

5. He Z. A linear source model and a unified rate control algorithm for DCT video coding / Z. He, S. K. Mitra // IEEE Transactions, Circuits and Systems for Video Technology. — 2002. — Vol. 12 (11). — P. 970–982.

6. Hsia S-C. A fast rate-distortion optimization algorithm for H.264/AVC codec / S-C. Hsia, W-C. Hsu, S-R. Wu // Signal, Image and Video Processing. — 2013. — Vol. 7 (5). — P. 939—949.

7. Kozhemiakin R. Peculiarities of 3D compression of noisy multichannel images / R. Kozhemiakin, S. Abramov, V. Lukin, I. Djurovic, B. Vozel // Procidings of Mediterranean Conference on Embedded Computing (MECO). — 2015. — P. 331–334.

8. Murtagh F. Astronomical image and signal processing / F. Murtagh, J. L. Starck // Signal Processing Magazine, IEEE. — 2001. — Vol. 18 (2). — P. 30–40.

9. Osokin A. N. Modified JPEG encoder with bit-rate control / A. N. Osokin, D.V. Sidorov / Online journal "Naukovedenie". — 2013. — 9 p.

10. Ponomarenko N. Image lossy compression providing a required visual quality / N. Ponomarenko, A. Zemliachenko, V. Lukin, K. Egiazarian, J. Astola // CD-ROM Proc. of the Seventh International Workshop on Video Processing and Quality Metrics for Consumer Electronics. — 2013. — 6 p.

11. Ponomarenko N. ADCT: A new high quality DCT based coder for lossy image compression / N. Ponomarenko, V. Lukin, K. Egiazarian, J. Astola // CD ROM Proceedings of LNLA. — Switzerland. — 2008. — 6 p.

12. Ponomarenko N. N. DCT Based High Quality Image Compression / N. N. Ponomarenko, V. V. Lukin, K. Egiazarian, J. Astola // Proceedings of 14th Scandinavian Conference on Image Analysis. — 2005. — Vol. 14. — P. 1177–1185.

13. Said A. A new fast and efficient image codec based on the partitioning in hierarchical trees/ A. Said // IEEE Trans. on Circuits Syst. Video Technology. — 1996. — Vol. 6. — P. 243–250.

14. Schowengerdt R. A. Remote Sensing: Models and Methods for Image Processing: Third edition / R. A. Schowengerdt / / Academic Press, San Diego. — 2006. — 560 p.

15. Skauli T. Sensor noise informed representation of hyperspectral data, with benefits for image storage and processing / T. Skauli // Optics Express. — 2011. — Vol. 19 (14). — P. 13031–13046.

16. Wallace G. K. The JPEG still picture compression standard / G. K. Wallace // Commun. ACM. — 1991. — Vol. 34. — P. 30–44.

17. Zemliachenko A. Lossy compression of noisy remote sensing images with prediction of optimal operation point existence and parameters / A. N. Zemliachenko, S. K. Abramov, V. V. Lukin, B. Vozel, K. Chehdi // Journal of Applied Remote Sensing. — 2015. — Vol. 9. — P. 095066–095066.

18. Zemliachenko A. N. Compression ratio prediction in lossy compression of noisy images / A. N. Zemliachenko, S. K. Abramov, V. V. Lukin, B. Vozel, K. Chehdi // Geoscience and Remote Sensing Symposium (IGARSS), IEEE International. — 2015. — P. 3497–3500.

19. Zemliachenko A. Lossy Compression of Hyperspectral Images Based on Noise Parameters Estimation and Variance Stabilizing Transform / N. Zemliachenko, A. Kozhemiakin, L. Uss, K. Abramov, N. Ponomarenko, V. Lukin, B. Vozel, K. Chehdi // Journal of Applied Remote Sensing. — 2014. — Vol. 8. — P. 1–25.

20. Zemliachenko A. Prediction of Compression Ratio in Lossy Compression of Noisy Images / A. Zemliachenko, R. Kozhemiakin, B. Vozel, V. Lukin // Modern Problems of Radio Engineering, Telecommunications and Computer Science (TCSET). — 2016. — 3 p.

21. Zhare A. Foreword to the Special Issue on Hyperspectral Image and Signal Processing / A. Zhare, J. Bolton, J. Cnanussot, P. Gader // IEEE Journal on Selected Topics in Applied Earth Observations and Remote Sensing. — 2014. — Vol. 7 (6). — P. 1841–1843.

МЕТОД ПРОГНОЗИРОВАНИЯ И ОБЕСПЕЧЕНИЯ КОЭФФИЦИЕНТА СЖАТИЯ ИЗОБРАЖЕНИЙ ДИСТАНЦИОННОГО ЗОНДИРОВАНИЯ ДЛЯ КОДЕРОВ НА ОСНОВЕ ДИСКРЕТНОГО КОСИНУСНОГО ПРЕОБРАЗОВАНИЯ

Р. А. Кожемякин, А. Н. Земляченко, В. В. Лукин, С. К. Абрамов, Б. Возель

Предложен и описан новый алгоритм предсказания коэффициента сжатия изображений дистанционного зондирования для кодера, основанного на дискретном косинусном преобразовании. Предложенный алгоритм является полностью автоматическим и простым, он обладает низкой вычислительной сложностью, что позволяет использовать его как на борту аэрокосмического аппарата, так и в пункте приема и обработки сигналов. Исследование проведено как для тестовых, так и для реальных изображений гиперспектральной системы Гиперион. Показано, что предложенный алгоритм обладает приемлемой точностью. Погрешность предсказания и обеспечения коэффициента сжатия или bpp не превышает 10%, что обычно достаточно для практического применения. Предложенный алгоритм работоспособен при разных уровнях помех.

**Ключевые слова:** дистанционное зондирование, ДКП кодеры, предсказание коэффициента сжатия, гиперспектральные данные

МЕТОД ПРОГНОЗУВАННЯ ТА ЗАБЕЗПЕЧЕННЯ КОЕФІЦІЄНТА СТИСНЕННЯ ЗОБРАЖЕНЬ ДИСТАНЦІЙНОГО ЗОНДУВАННЯ ДЛЯ КОДЕРІВ НА ОСНОВІ ДИСКРЕТНОГО КОСИНУСНОГО ПЕРЕТВОРЕННЯ

Р. О. Кожемякін, О. М. Земляченко, В. В. Лукін, С. К. Абрамов, Б. Возель

Запропоновано і описано новий алгоритм прогнозування коефіцієнта стиснення зображень дистанційного зондування для кодерів, заснованих на дискретному косинусному перетворенні. Запропонований алгоритм є автоматичним і простим, він має низьку обчислювальну складність, що дозволяє використовувати його як на борту аерокосмічного апарату, так і в пункті прийому і обробки сигналів. Дослідження проведене як для тестових, так і для реальних зображень гіперспектральної системи Гіперіон. Показано, що запропонований алгоритм має прийнятну точність. Похибка передбачення та забезпечення коефіцієнта стиснення або bpp не перевищує 10%, що зазвичай достатньо для практичного застосування. Запропонований алгоритм працездатен при різних рівнях перешкод.

**Ключові слова:** дистанційне зондування, ДКП кодери, прогнозування коефіцієнта стиснення, гіперспектральні дані